Int. J. Heat Mass Transfer. Vol. 34, No. 2, pp. 573–578, 1991
Printed in Great Britain

0017–9310/91 $3.00 + 0.00

TECHNICAL NOTES

Convection in a vertical channel with a finite wall heat source

D. ELPIDOROU, V. PRASAD† and V. MODI
Department of Mechanical Engineering, Columbia University, New York, NY 10027, U.S.A.

(*Received* 6 *November* 1989 *and in final form* 20 *March* 1990)

1. INTRODUCTION

FREE AND forced convection in a vertical channel with one or both of the walls uniformly heated has been studied extensively owing to its importance in several engineering applications. Both symmetric as well as asymmetric heating either at constant temperature(s) or by uniform heat flux(es) have been considered [1, 2]. Convection from discrete heat sources located on one of the walls of a vertical channel has been investigated only in recent years. An excellent review of these studies has been presented recently by Moffat and Ortega [2]. As this review article indicates, most of these studies consider protruded heat sources that are either two-dimensional (strip heating) or three-dimensional (discrete sources in several rows). However, there has been only a limited effort towards understanding the more fundamental problem of convective flows and heat transfer in a channel with one or more flush-mounted heat sources.

Although free convection heat transfer either from a single or multiple flush-mounted, discrete heat source on a vertical plate has been studied both numerically as well as experimentally [3], the channel problem has been considered by only Ravine and Richards [4]. They found that the heat transfer from a horizontal strip on one vertical wall which is otherwise adiabatic, is less than that from an unshrouded vertical plate [5]. They reported 20–30% reduction in heat transfer due to shrouding. This is in contrast to the observation made by Ortega and Moffat [6] who observed an increase in free convection heat transfer from an array of cubical elements mounted on a vertical plate when the plate was shrouded. The present work is a numerical study of the problem of free convection from a discrete heat source in a vertical channel originally considered by Ravine and Richards [4]. The effects of forced flow on buoyancy-induced velocity and temperature fields, and the heat transfer rates are also examined. The computations are restricted to a vertical channel the width of which is equal to the height of the heating element, and the Prandtl number is held constant at 0.707.

2. FORMULATION AND NUMERICAL METHOD

Consider a two-dimensional vertical channel in which a flush-mounted, isoflux heat source of width ($H = W$), is located on one of the vertical walls that is otherwise adiabatic. The other vertical wall of the channel is maintained either at a constant temperature or is insulated. The flow of air at a temperature T_c, through the bottom end of the channel may be caused due to the buoyancy forces or an externally-imposed pressure gradient, or both. The thermophysical properties of air ($Pr = 0.707$) are assumed to be constant and the flow is considered to be incompressible. With these assumptions the governing equations may be transformed into the dimensionless form of stream function–vorticity–temperature equations in the usual way

$$\nabla^2\psi = -\zeta \tag{1}$$

$$\frac{\partial\zeta}{\partial t} + u\frac{\partial\zeta}{\partial X} + v\frac{\partial\zeta}{\partial Y} = \frac{Gr}{Re^2}\frac{\partial\theta}{\partial X} + \frac{1}{Re}\left(\frac{\partial^2\zeta}{\partial X^2} + \frac{\partial^2\zeta}{\partial Y^2}\right) \tag{2}$$

$$\frac{\partial\theta}{\partial t} + u\frac{\partial\theta}{\partial X} + v\frac{\partial\theta}{\partial Y} = \frac{1}{Re\,Pr}\left(\frac{\partial^2\theta}{\partial X^2} + \frac{\partial^2\theta}{\partial Y^2}\right) \tag{3}$$

where the Boussinesq approximation has been invoked. Equations (1)–(3) reduce to a set of governing equations for free convection when Re is taken as unity; the velocity scale then reduces to v/H.

The relevant boundary conditions for the channel walls may be written as

$$X = 0, \quad \psi = 0, \quad \partial^2\psi/\partial X^2 = 0;$$
$$\partial\theta/\partial X = -1 \quad 0 < Y < H$$
$$\partial\theta/\partial X = 0 \quad Y < 0 \text{ and } Y > H \tag{4}$$

$$X = W/H, \quad \psi = \psi_{max}, \quad \partial^2\psi/\partial X^2 = 0,$$
$$\theta = 0 \quad \text{or} \quad \partial\theta/\partial X = 0 \quad 0 \leqslant Y \leqslant 1 \tag{5}$$

where ψ_{max} depends on the mode of convection. In the case of forced convection, ψ_{max} can be taken as unity while for free convection, ψ_{max} is obtained from the mass balance between the inlet and exit flow rates which requires an iterative procedure. In the case of mixed convection, ψ_{max} is computed by superimposing the forced flow over the free convection velocity solutions. Hence, the buoyancy-induced flow is solved first for various Grashof numbers and then the computations are performed for mixed convection problems. To reduce the CPU time for steady-state solutions, the flow rate obtained from the boundary layer solutions for a vertical plate, is used to calculate the initial value of $\psi_{max}(Gr)$. The conditions at the inlet and exit are, however, not easy to specify. If the ends are considered to be sufficiently far from the heat source, such that the inflow and outflow can be assumed parallel and axial conduction can be neglected, the exit boundary conditions are

$$u = \partial\psi/\partial Y = 0, \quad \partial v/\partial Y = -\partial^2\psi/\partial X\partial Y = 0, \quad \partial\theta/\partial Y = 0. \tag{6}$$

To choose an appropriate set of boundary conditions at the inlet, the computations were performed for the following set of conditions:

$$\psi = -X \times V_m, \quad \zeta = 0 \text{ or } \partial\zeta/\partial Y = 0, \quad \theta = 0 \tag{7a}$$

$$\partial\psi/\partial Y = 0, \quad \zeta = 0 \text{ or } \partial\zeta/\partial Y = 0, \quad \theta = 0. \tag{7b}$$

Interestingly, the variations in Nu and ψ_{max} were found to be very small. However, the streamline patterns produced by boundary conditions (7a) with $\zeta = 0$ looked more realistic, and hence that condition was adopted for the computations reported here. The effects of inlet boundary conditions are

† Author to whom correspondence should be addressed.

NOMENCLATURE

g	acceleration due to gravity [m s^{-2}]
Gr	Grashof number, $(g\beta q'' H^4)/(kv^2)$
h_y	local heat transfer coefficient, $q''/(T-T_c)$ [W m^{-2} K^{-1}]
$\bar{h}$	average heat transfer coefficient, $q''/(T_{h,m}-T_c)$ [W m^{-2} K^{-1}]
H	width of the heat source [m]
k	thermal conductivity [W m^{-1} K^{-1}]
Nu_m	average Nusselt number, $\bar{h}H/k = 1/\theta_m$
Nu_y	local Nusselt number, $h_y y/k = Y/\theta$
Pr	Prandtl number, v/α
q''	uniform heat flux [W m^{-2}]
Re	Reynolds number, VH/v
t	dimensionless time
T	temperature [K]
u, v	dimensionless velocity in x- and y-directions
V	forced flow velocity ($=v/H$ for free convection) [m s^{-1}]
W	width of the channel [m]
X, Y	dimensionless distance in the x- and y-directions, x/H and y/H.

Greek symbols

α	thermal diffusivity [m^2 s^{-1}]
β	isobaric coefficient of expansion [K^{-1}]
ζ	dimensionless vorticity, $(\partial v/\partial X - \partial u/\partial Y)$
θ	dimensionless temperature, $(T-T_c)/(q''H/k)$
v	kinematic viscosity [m^2 s^{-1}]
ψ	dimensionless stream function, $u = \partial\psi/\partial X$ and $v = -\partial\psi/\partial Y$.

Subscripts

c	inlet condition
h	heated segment
m	mean value
max	largest value
y	local value, based on y as length scale.

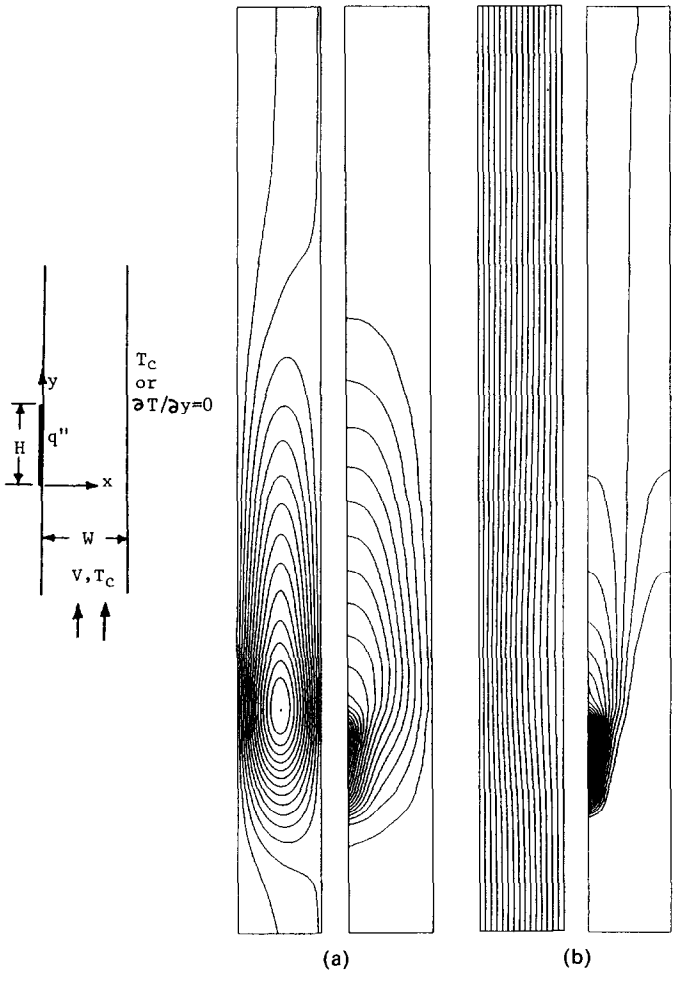

FIG. 1. Effect of opposite wall boundary conditions, (a) isothermally cooled and (b) adiabatic, on buoyancy-induced flow and temperature fields in a vertical channel ($Gr = 10^4$).

discussed in detail by Ramanathan and Kumar [7], among others.

In the present numerical scheme, equations (1)–(3) are discretized by employing central differences for spatial derivatives and forward differences for time derivatives. An ADI procedure is used to perform the time integration of vorticity and temperature equations while the stream function equation is solved by a Gauss–Seidel SOR point iterative scheme at each time step. Solutions are considered to be steady when the fractional changes in ζ and θ between two time steps is less than 10^{-4} at each node. The iterative convergence of stream function is checked by obtaining the fractional difference between two successive values of $\psi < 10^{-3}$. For free convection solutions, the iterations for mass balance are carried out unless the change in V_m is less than 0.1%.

To determine an appropriate grid field, computations were performed for 21×99 to 31×121 nodes. A 31×105 mesh with a uniform grid in the x-direction and a non-uniform grid in the y-direction is found to be the best compromise between accuracy and CPU time. The ratio of height to the width of the channel was taken as 11 with an adiabatic segment of two heater lengths on the upstream side. The nodes in the y-direction were distributed in such a way that the leading and trailing edges of the heat source fall at midpoints of the respective grids. Very small time steps (of the order of 10^{-3}) were used to overcome the difficulty of numerical instability. The accuracy of the numerical results was first verified by performing calculations for a differentially-heated vertical cavity. To further check the reliability of the present results, an overall energy balance was employed for the system. This compared the heat input with the energy leaving the channel, and was satisfied within 2–5%.

3. RESULTS AND DISCUSSION

Numerical results have been obtained for free and forced convection for $10^3 \leqslant Gr \leqslant 10^6$ and $10 \leqslant Re \leqslant 2000$, respectively. Mixed convection calculations, on the other hand, are performed for $Gr = 10^4$, 10^5, and 5×10^5 and $10 \leqslant Re \leqslant 2000$.

3.1. *Flow and temperature fields*

Figure 1(a) presents the streamlines and isotherms for free convection in a vertical channel the right-hand wall of which is isothermal. A recirculatory motion is induced by the isolated heat source since the opposite wall acts as a heat sink. Hence, the flow of air through the channel is very weak, and a large fraction of heat is rejected on the cold wall. Indeed, the through flow of air will further weaken if the heat source is located further away from the inlet. This

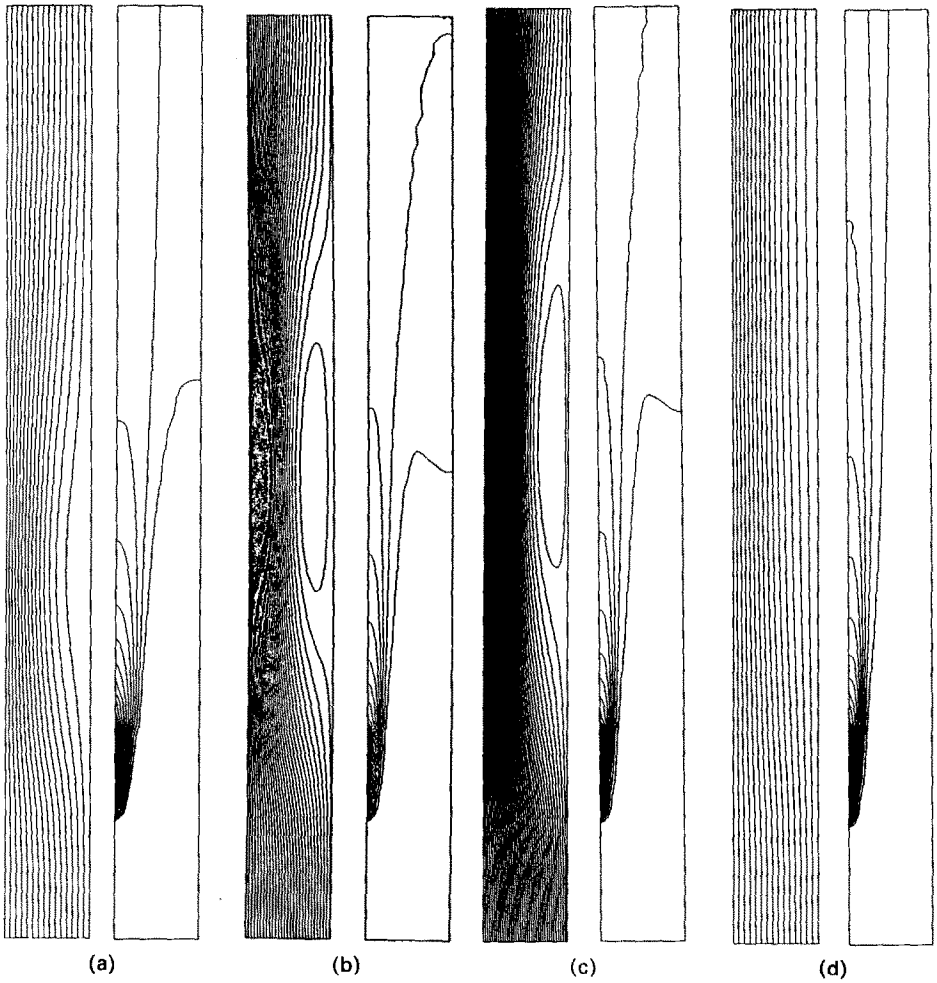

FIG. 2. Velocity and temperature fields for natural convection, (a) $Gr = 10^5$, (b) $Gr = 5 \times 10^5$, and mixed convection, (c) $Gr = 5 \times 10^5$, $Re = 10$, (d) $Gr = 5 \times 10^5$, $Re = 100$.

behavior has been well demonstrated by the numerical work of Lai *et al.* on free convection from a finite wall heat source in a channel filled with a saturated porous medium [8]. It is obvious that the higher the Grashof number, the stronger will be the recirculating flow and the larger the extent of the convective cell. For these boundary conditions, the convective cell will extend much more on the upper side of the heat source than below it which indicates the possibility of flow entrainment at the exit if the channel is short.

The recirculating flow, however, vanishes if the opposite wall is considered to be adiabatic and the Grashof number is kept constant, $Gr = 10^4$ (Figs. 1(a) and (b)). The flow is now almost parallel and the thermal diffusion is comparable to convection. Also, the induced flow is much stronger than that observed in the previous case. Interestingly, as the Grashof number is increased, the acceleration caused by the buoyant forces deflects the flow toward the heat source causing a separation from the right adiabatic wall (Figs. 1(b), 2(a) and (b)). The vertical velocity near the heat source thus increases, and the convective effect on the downstream side is enhanced. The aiding flow, however, reattaches to the right-hand wall far downstream (away from the heat source) once the (gained) heat has been sufficiently distributed over the entire width of the channel. The horizontal temperature gradient on the downstream side beyond the recirculating flow region, is then very weak. It is also interesting to note that the recirculating cell moves further away from the heat source as the Grashof number is increased. Clearly, the separation and reattachment, and the flow entrainment at the exit, if any, are complex functions of the strength of the heat source, the length of the vertical channel, particularly on the downstream side, and the thermal boundary condition on the shrouding wall.

On the other hand, the forced flow has a stabilizing effect on the buoyancy-induced flow field. Figures 2(b) and (c) show that the convective cell acts like a bubble and is moved up as the flow rate is increased which may be caused by an increase in either the buoyancy effects or forced flow velocity, or both. The recirculating flow for $Gr = 5 \times 10^5$ finally vanishes at $Re \cong 100$ (Fig. 2(d)). The heat transfer is now strongly convection dominated, and the horizontal temperature gradient particularly in the left-hand wall region, is strong even at a distance far away from the heat source. The isotherms in Fig. 2(d) also indicate that the presence of the right adiabatic wall has a minimal effect on the thermal field. A small deviation from the parallel flow as displayed in Fig. 2(d) is eliminated completely when the Reynolds number is about 500. A similar behavior was demonstrated by the streamline and isotherm patterns for other Grashof numbers. As can be expected, the Reynolds number required to stabilize the flow decreases with Grashof number.

The maximum temperature, θ_{max}, which occurs near the trailing edge of the heat source is presented in Fig. 3(a) and Table 1 for free convection. The θ_{max} vs Gr plot is a straight line and can be correlated as

$$(\theta_{max})_{NC} = 0.997 Gr^{-0.148} \tag{8}$$

which predicts the numerical data within 4%. Figure 3(a) and equation (8) show that θ_{max} decreases with an increase in Grashof number. However, from the definition of θ and Gr, it is clear that T_{max} increases with the heat flux, and $(T_{max} - T_c) \propto q''^{0.852}$. It should be noted that θ_{max} occurs at $Y \approx 1$ only at high Grashof numbers. At low values of Gr, the location of θ_{max} moves away from the trailing edge and may be as low as $X \approx 0.85$ at $Gr = 10^3$. This is primarily because of thermal diffusion being significant at low Grashof numbers.

For forced convection at a low Reynolds number

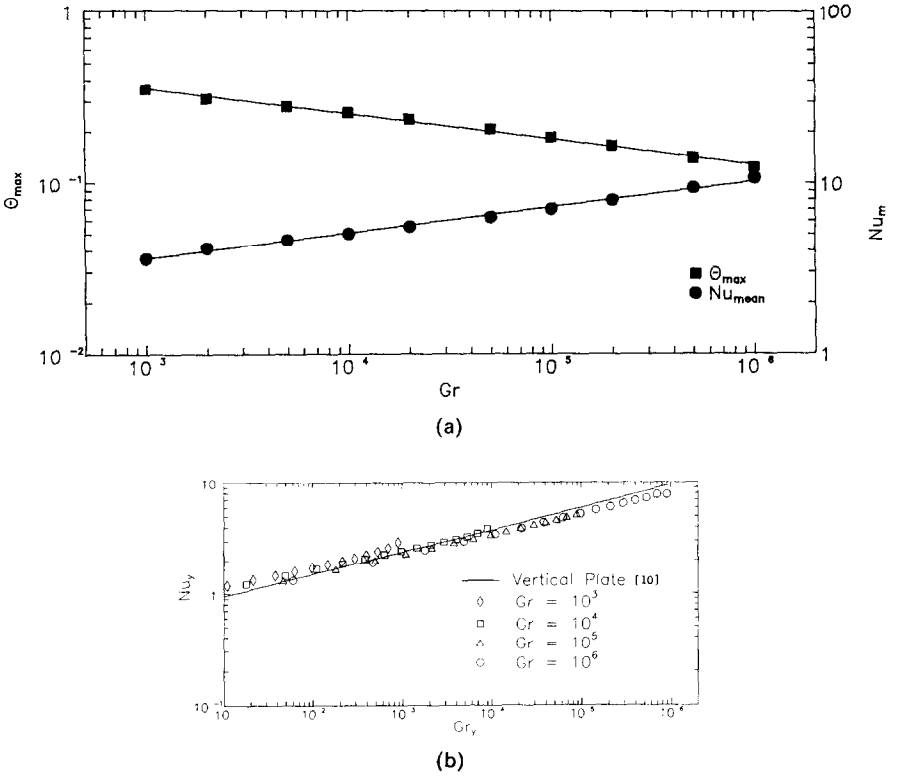

FIG. 3. (a) Maximum temperature θ_{max} and mean Nusselt number as functions of Grashof number, and (b) local Nusselt number for free convection in a channel of adiabatic walls and a discrete heat source on one wall.

Table 1. Maximum temperature on the heated segment, θ_{max}, and its location

Gr	Natural convection	Re 10	50	100	200	500	1000	2000
5×10^5	0.142	0.137	0.133	—	0.121	0.100	0.080	0.061
10^5	0.186	0.181	0.168	—	0.135	0.104	0.081	0.061
10^4	0.260[c]	0.244[c]	0.204[c]	—	0.144[c]	0.106	0.082	0.061
Forced convection		0.422[a]	0.249[b]	0.198[c]	—	—	0.083	0.062

Location for θ_{max}: [a] $Y \cong 0.79$; [b] $Y \cong 0.87$; [c] $Y \cong 0.91$ and the rest at $Y \cong 0.98$.

($Re = 10$), the largest temperature on the heated segment is about 25% higher than the mean temperature, and occurs at $Y \cong 0.8$ (Table 1). However, the ratio $(\theta_{max}/\theta_m)_{FC}$ increases to 1.47 as the Reynolds number is increased to 2000. The location for θ_{max} in this case is very close to the trailing edge, $Y \cong 0.98$. In the case of mixed convection $(\theta_{max}/\theta_m)_{MC}$ varies between 1.33 and 1.48 for the computed range of Grashof and Reynolds numbers with the location at which θ is largest being very close to the trailing edge ($Y \cong 0.97$) except when both Re and Gr are small.

3.2. *Free convection heat transfer*

The local heat transfer rate for free convection is reported in Fig. 3(b) together with the vertical plate solution of Vliet [9]. As can be seen, the local Nusselt number, Nu_y, is about 25% higher than that for the vertical plate when $Gr = 10^3$. However, this trend reverses with an increase in buoyancy forces, and Nu_y for $Gr = 10^6$ decreases below Vliet's results, the difference being as high as 16%. These data can be correlated as

$$(Nu_y)_{NC} = 0.726Gr^{0.17} \tag{9}$$

with the largest variations of $\pm 20\%$. Figure 3(a), on the other hand, presents the mean Nusselt number as a function of channel Grashof number, Gr, which can be correlated as

$$(Nu_m)_{NC} = 1.253Gr^{0.152} \tag{10}$$

with $\pm 4\%$ deviation from the computed values.

It is evident from equations (9) and (10) that the slope of Nusselt vs Grashof numbers curve is not identical to what has been reported for the vertical plate, 0.2064 for discrete heating [5] and 0.2 for the uniformly heated case [7, 9, 10]. This agrees with the observation of Ravine and Richards [4] to the extent, that the slope of the Nusselt number curve changes when the plate with a discrete heat source is shrouded. Figures 3(a) and (b) further demonstrate that the heat transfer rate increases due to shrouding at low Grashof number ($Gr < 2\times10^4$). In this range of Grashof number, the present numerical results support the theory of Ortega and Moffat and others [2, 6] that the combined effects of local buoyancy and forced convection from the induced flow result in higher Nusselt numbers for a discrete heat source. However, the enhancement is not as dramatic as these authors have reported which may have been caused by the protrusion effects in their geometry.

It should be noted that the experimental data of Ravine and Richards [5] showed a reduction in heat transfer at all Grashof numbers, when compared to a vertical plate. We have, however, found that their experimental values of Nu_y for $W/H = 0.962$ are about 20–30% lower than the predicted heat transfer rates for $W/H = 1$. This reduction may have been caused by the heat loss from unheated sections of the channel which would reduce the overall buoyancy forces and therefore the chimney effect, as also argued by Moffat and Ortega [2].

Interestingly, our numerical results at high Grashof numbers support the conclusion drawn by Ravine and Richards that the enhancement due to the induced duct flow may not always compensate for the reduction in heat transfer due to the loss of unrestricted entrainment from the surroundings. It is thus concluded that the free convection heat transfer in a discretely heated channel will exceed that for a vertical plate only under special circumstances determined by the channel width, heater protrusion, Grashof number and so on.

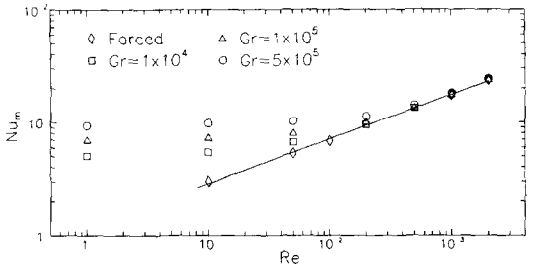

FIG. 4. Nusselt numbers for mixed and forced convection.

Furthermore, if an attempt is made to predict the free convection Nusselt numbers by employing the forced convection correlation (equation (11)) following Moffat and Ortega [2], we find that the predicted values of Nu_m are substantially lower than the computed Nusselt numbers. The variation of 6.6% at $Gr = 10^3$ increases to 59% at $Gr = 10^6$.

3.3. *Forced convection*

The computed Nusselt numbers for forced convection heat transfer are presented in Fig. 4, and can be correlated as

$$(Nu_m)_{FC} = 1.166Re^{0.393} \tag{11}$$

which predicts the numerical data to within $\pm 4.5\%$. Our Nusselt numbers for forced convection are generally lower than that predicted by the correlation for a uniformly heated plate with no unheated length [11]. The variation is almost zero at $Re = 30$, but increases to about 33% at $Re = 2000$. On the other hand, we predict higher heat transfer rates at $Re < 30$. Clearly, the unheated inlet and exit sections, and shrouding considered in the present problem contribute to this difference.

If we compare our local Nusselt numbers with those reported by Heaton *et al.* [12] for developing laminar flow of air through an asymmetrically heated channel, we find that the present values are consistently lower than that for a channel of length H with no adiabatic inlet and exit sections. The difference is substantial at small Reynolds number and near the leading edge (42% at $X = 0.028$ for $Re = 10$), but diminishes as X and Re increase.

3.4. *Mixed convection*

The Nusselt numbers for mixed convection heat transfer are presented in Fig. 4 for $Gr = 10^4$, 10^5 and 5×10^5. Clearly, the effect of buoyancy forces are negligible at $Re > 500$ for all Grashof numbers ($Gr \leqslant 5\times10^5$). A general criterion for the forced convection dominant heat transfer is $Gr/Re^2 < 2$, based on about 5% variation in Nusselt numbers. When compared with the criterion presented by Moffat and Ortega [2], we find that our value of Gr/Re^2 is on the higher side. The present numerical data do not yield any criterion for a free convection dominant regime. However, the computed values of mixed convection Nusselt number are surprisingly close (within 3%) of the predictions made by a composite

relation based on free and forced convection

$$[Nu_{MC}]^n = [Nu_{NC}]^n + [Nu_{FC}]^n, \quad n = 3. \tag{12}$$

4. CONCLUSION

Numerical results have been reported for two-dimensional, steady free, forced and mixed convection from a flush-mounted, isoflux heat source on one vertical wall of the channel the walls of which are otherwise adiabatic. In the free convection regime, the flow may separate from the unheated wall at high Grashof numbers, and if the channel is long, it may reattach at a distance far away from the heat source. The recirculating flow, however, disappears as the Reynolds number increases. The strength and extent of the convective cell depend strongly on Grashof and Reynolds numbers and show the possibility of flow entrainment at the exit end if the channel is short.

The heat transfer rate is also a strong function of Grashof and Reynolds number. Depending on the Grashof number, it may be either lower or higher than the vertical plate solutions. However, in the forced convection regime, it is always lower than the flat plate results. The mixed convection Nusselt numbers can be easily predicted by a composite relation based on the free and forced convection values (equation (14)). The present problem, however, does not fall into the category for which free and mixed convection Nusselt numbers can be predicted from the forced convection correlations as proposed by Ortega and Moffat for discretely heated channels [2]. Also, these results neither support the theory that the Nusselt numbers for the present problem are always lower than the vertical plate solutions in the free convection regime, nor do they agree with the observation of several authors that the discrete heating always results in higher heat transfer rates. Finally, we expect that numerical results reported here will provide a basis for better understanding of the effects of shrouding and wall protuberances, as well as the influence of both the upstream and downstream adiabatic sections.

REFERENCES

1. A. D. Kraus and A. Bar-Cohen, *Thermal Analysis and Control of Electronic Equipment*, pp. 303–320. Hemisphere, New York (1983).
2. R. J. Moffat and A. Ortega, Direct air cooling of electronic components. In *Advances in Thermal Modelling of Electronic Components and Systems* (Edited by A. Bar-Cohen and A. D. Kraus), pp. 129–262. Hemisphere, New York (1988).
3. Y. Jaluria, Natural convection cooling of electronic equipment. In *Natural Convection: Fundamentals and Applications* (Edited by S. Kakac *et al.*), pp. 961–986. Hemisphere, New York (1985).
4. T. L. Ravine and D. E. Richards, Natural convection heat transfer from a discrete thermal source on a channel wall, *J. Heat Transfer* **110**, 1004–1007 (1988).
5. T. L. Ravine and D. E. Richards, Natural convection heat transfer from a discrete thermal source on a vertical surface, *J. Heat Transfer* **110**, 1007–1009 (1988).
6. A. Ortega and R. J. Moffat, Heat transfer from an array of simulated electronic components: experimental results for free convection with and without a shrouding wall. In *Heat Transfer in Electronic Equipment—1985* (Edited by S. Oktay and R. J. Moffat), ASME-HTD Vol. 48, pp. 5–15 (1985).
7. S. Ramanathan and R. Kumar, Correlations for natural convection between heated vertical plates, *Proc. ASME Winter Annual Meeting* (1988); also in *J. Heat Transfer* (in press).
8. F. C. Lai, V. Prasad and F. A. Kulacki, Aiding and opposing mixed convection in a vertical porous layer with a finite wall heat source, *Int. J. Heat Mass Transfer* **31**, 1049–1061 (1988).
9. G. C. Vliet, Natural convection local heat transfer on constant heat-flux inclined surfaces, *J. Heat Transfer* **91**, 511–516 (1969).
10. R. A. Wirtz and R. J. Stutzman, Experiments on free convection between vertical plates with symmetric heating, *J. Heat Transfer* **104**, 501–507 (1982).
11. W. M. Kays and M. E. Crawford, *Convective Heat and Mass Transfer*, 2nd Edn. McGraw-Hill, New York (1980).
12. H. S. Heaton, W. C. Reynolds and W. M. Kays, Heat transfer in annular passages. Simultaneous development of velocity and temperature fields in laminar flow, *Int. J. Heat Mass Transfer* **7**, 763–781 (1964).

Int. J. Heat Mass Transfer. Vol. 34, No. 2, pp. 578–582, 1991
Printed in Great Britain

0017-9310/91 $3.00 + 0.00

Film condensation on an upward facing plate with free edges

ADRIAN BEJAN
Department of Mechanical Engineering and Materials Science, Duke University, Durham, NC 27706, U.S.A.

(*Received* 12 *December* 1989 *and in final form* 20 *April* 1990)

INTRODUCTION

THE PURPOSE of this note is to report several laminar film condensation results that apply to a basic geometric configuration—the plane horizontal surface that faces upward. Reviews of the laminar film condensation field [1–3] have shown that solutions have been developed for a wide variety of wall shapes and orientations, e.g. vertical and inclined plates, horizontal and inclined cylinders, a sphere, and several types of rotating surfaces. It has been recognized also that the phenomenon of condensation on a horizontal flat surface can behave in more than one way, depending on whether the surface faces upward or downward. The case of the downward facing plate was treated by Gerstmann and Griffith [4], who showed that the condensate film develops a bumpy surface (cf. the Taylor instability) from which droplets leave the film intermittently.

The upward facing plate is discussed by Rohsenow [1], but only under the assumption that the plate serves as the bottom surface for a vessel with adiabatic vertical walls. In that case, the lateral walls prevent the horizontal motion of the condensate, and the time-dependent growth of the film thickness is described by the one-dimensional (vertical) conduction solution associated with the classical Stefan problem.